

1 **Climate, Air Quality and Human Health Benefits of Various Solar Photovoltaic**  
2 **Development Scenarios in China in 2030**

3 **Supporting Information (SI)**

4 Junnan Yang<sup>1</sup>, Xiaoyuan Li<sup>2</sup>, Wei Peng<sup>1,3</sup>, Fabian Wagner<sup>4</sup>, and Denise L. Mauzerall<sup>1,2</sup>

5 <sup>1</sup>Woodrow Wilson School of Public and International Affairs, Princeton University,  
6 Princeton, NJ 08544, United States of America

7 <sup>2</sup>Department of Civil and Environmental Engineering, Princeton University, Princeton, NJ  
8 08544, United States of America

9 <sup>3</sup>Now at Belfer Center for Science and International Affairs, Harvard Kennedy School,  
10 Cambridge, MA 02138, United States of America

11 <sup>4</sup>International Institute for Applied Systems Analysis (IIASA), Laxenburg, Austria

12 1. China's regional power grids



13

14 **Fig. S1.** China's six regional power grids (excluding Tibet)

15 **2. Detailed methods for calculating capacity factors for both types of PV for each**  
16 **province**

17 We apply the PVLIB-Python model, a solar PV performance model, to simulate PV  
18 electricity generation efficiencies at each 1° latitude by 1° longitude continental grid box  
19 globally. PVLIB-Python takes irradiance data as input and provides alternating current  
20 (AC) power as output. We further calculate PV capacity factors (the AC output divided  
21 by the designed maximum output power) to measure PV efficiency. We use surface solar  
22 irradiance from the NASA CERES-SYN1deg dataset including both clouds and aerosols.

23 The model takes input of surface solar irradiance, first calculates the point-of-array-  
24 irradiance (POAI, irradiance received by a panel at any tilted angle), further takes the  
25 input of weather data to calculate the direct-current (DC) output power, and finally  
26 applying the inverter for the AC output power. In this process, both PV cell efficiency  
27 (solar energy converted to DC electricity) and inverter efficiency (DC to AC electricity)  
28 are considered. We applied the wrapper developed by Li et al. (2017) [1], which enables  
29 parallel computing for a large number of grid-point locations and time steps using the  
30 PVLIB-Python model, and increases the computing efficiency.

31 In this study, Canadian Solar CS5P 220M is used as the PV module, with maximum  
32 output power of 220 W and peak efficiency of 12.94%. ABB MICRO-0.25-I-OUTD-US  
33 208Vac is the inverter applied to the model with designed efficiency of 96%. Combined  
34 together, the peak PV system efficiency is 12.42%.

35 **3. Detailed methods for determining the order of coal-fired power plant**  
36 **displacement in the *Regional* scenarios**

37 In the *Regional* scenarios, we determine the order of subcritical coal power plant  
38 displacement by the damage-weighted PM<sub>2.5</sub> precursor emissions calculated as

39 
$$EF_{eff,j}^i = (1.75 \times EF_{SO_2,j}^i + EF_{NO_x,j}^i) \quad (1)$$

40  $EF_{eff,j}^i$  is the effective emission factor for the specific category of coal-fired power plant  
41  $j$  in province  $i$  (unit: kt/PJ)

42  $EF_{SO_2,j}^i$  is the SO<sub>2</sub> emission factor for the specific type of coal-fired power plant  $j$  in  
43 province  $i$  (unit: kt/PJ)

44  $EF_{NO_x,j}^i$  is the NO<sub>x</sub> emission factor for the specific type of coal-fired power plant  $j$  in  
45 province  $i$  (unit: kt/PJ).

46 The emission factors for SO<sub>2</sub> and NO<sub>x</sub> are from the ECLIPSE\_v5a\_CLE scenario in the  
47 Greenhouse Gas and Air Pollution Interactions and Synergies (GAINS) model. For each  
48 air pollutant, subcritical coal plants are further disaggregated into different categories  
49 according to the end-of-pipe control technologies they employ in GAINS and presented  
50 as the percentages of total coal use for electricity generation. The 1.75 weighting is  
51 obtained from a related study to the health impacts of SO<sub>2</sub> and NO<sub>x</sub> from the power  
52 sector, considering their relative contributions to the formation of secondary inorganic  
53 aerosols [2].

#### 54 **4. Detailed methods on spatial and temporal allocations of emissions in the base** 55 **case and PV scenarios**

56 We map provincial annual emissions in the ECLIPSE\_v5a\_CLE scenario and all four PV  
57 scenarios onto gridded (0.25 degree by 0.25 degree) and monthly emission profiles  
58 following the spatial and temporal patterns from the MEIC 2012 emission inventory. In  
59 detail, for each province  $i, i \in [1,31]$  in China, each sector  $j, j \in [1,5]$  (power, industry,  
60 transportation, residential, and agriculture) and each month  $m, m \in [1,12]$ , there are  
61 gridded (0.25 degree by 0.25 degree) MEIC emissions for each pollutant ( $MEIC_{i,j,m}^k$ ,  $k$   
62 represents all grid boxes that belong to Province  $i$ ). There are also annual emissions in  
63 MEIC for each grid box for each pollutant ( $MEIC_{i,j,a}^k$ ,  $a$  means annual total emission).

64 In the GAINS emission inventory there are only annual provincial total emissions for  
65 each sector ( $GAINS_{i,j,a}^{Base}$  for the base case emissions). In particular, coal-fired power  
66 plants in GAINS are divided into 18 different categories based on their efficiency levels  
67 and air pollutant emission factors (unit: g/kWh electricity generated). The  
68 ECLIPSE\_v5a\_CLE scenario does not have a plant-level database of all coal-fired power  
69 plants, thus only the aggregated electricity generation data in each category is provided in  
70 the GAINS model. In the four PV scenarios, we calculate the annual provincial total  
71 emissions for each pollutant ( $GAINS_{i,j,a}^{Sce}$ ) by subtracting the sum of emissions from the  
72 coal plants that are displaced by PV in each category in the base case ( $GAINS_{i,j,a}^{Base}$ ). The  
73 emissions of each pollutant from those displaced coal plants are calculated as the product  
74 of the electricity generated from those coal plants in the base case and the emission  
75 factors of each pollutant. We displace coal plants from the category with the most  
76 polluting (defined as the highest  $SO_2$  and  $NO_x$  emissions combined) subcritical coal-fired  
77 power plants to the category with the least polluting coal plants. The most polluting  
78 subcritical coal plants are also the least efficient ones, and have the highest  $CO_2$  emission  
79 factor accordingly. To get the gridded monthly GAINS emissions, we assume that the  
80 GAINS emissions follow the same spatial and temporal pattern as MEIC and calculate  
81 the gridded emissions using Equations (2) and (3).

82 
$$GAINS_{i,j,m}^{Base,k} = MEIC_{i,j,m}^k \times \frac{GAINS_{i,j,a}^{Base}}{\sum_k MEIC_{i,j,a}^k} \quad (2)$$

83 
$$GAINS_{i,j,m}^{Sce,k} = MEIC_{i,j,m}^k \times \frac{GAINS_{i,j,a}^{Sce}}{\sum_k MEIC_{i,j,a}^k} \quad (3)$$

84 We use the same methods for emissions outside China, where we map the annual  
85 country-specific emissions in ECLIPSE\_v5a\_CLE onto gridded (0.1 degree by 0.1  
86 degree) monthly profiles following the spatial and temporal patterns from the HTAP  
87 2010 emission inventory.

88 **5. More details on WRF-Chem model configurations:**

89

90

**Table S1.** Physical and chemistry options used in WRF-Chem simulation

Model configurations	
Atmospheric process	WRF-Chem scheme
Cloud microphysics	Lin et al. scheme
Long-wave radiation	RRTM scheme
Short-wave radiation	Goddard shortwave
Surface layer	MM5 similarity
Boundary layer	Yonsei University scheme
Cumulus parameterization	Grell 3D scheme
Land surface	Noah land surface model
Chemistry option	RADM2 chemical mechanisms and MADE/SORGAM aerosols including aqueous chemistry
Photolysis	Fast-J photolysis

91 **6. Detailed calculations of health impacts associated with air pollution**

92 Changes in the number of premature deaths of each disease associated with PM<sub>2.5</sub> pollution  
93 in each 27 km by 27 km WRF-Chem grid box are calculated as follows:

94 
$$\Delta Mort_i = POP * MR_{Base,i} * [RR_i(C_{Sce}) / RR_i(C_{Base}) - 1] \quad (4)$$

95  $\Delta Mort_i$  is the change in premature mortalities in each WRF-Chem grid box due to disease  
96  $i$  in 2030;

97  $POP$  is the projected population in each grid in 2030 (total provincial population is  
98 included in the Eclipse\_v5a\_CLE scenario, county-level population distribution follows  
99 the same pattern as the 2010 China census data [3]. We use ArcGIS 10.0 to map county-  
100 level population onto WRF-Chem grid boxes).

101  $MR_{Base,i}$  is the baseline mortality rate for disease  $i$  in 2013 [4],

102  $RR(C_{Sce})$  is the relative risk (RR) for disease  $i$  at the PM<sub>2.5</sub> concentration (C) in each  
103 scenario ( $Sce$ ). We use RR functions from the Global Burden of Disease study (3), with  
104 linear interpolations for non-integer concentration levels,

105  $RR(C_{Base})$  is the relative risk for disease  $i$  at the PM<sub>2.5</sub> concentration in the base case.

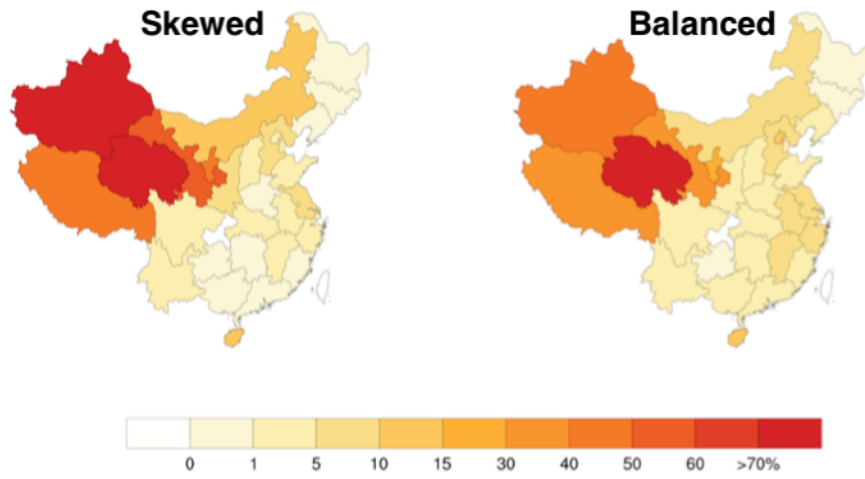
106 **7. Comparison of capacity factors obtained with one-axis tracking systems applied**  
 107 **in utility-scale PV plants and those obtained with fixed arrays in distributed PV**  
 108 **systems by province**

109 **Table S2.** Capacity factors of utility-scale and distributed PV by province

Province	Capacity factors for utility-scale PV	Capacity factors for distributed PV
Anhui	0.1437	0.1393
Beijing	0.1998	0.1907
Chongqing	0.1159	0.1103
Fujian	0.1426	0.1413
Gansu	0.2208	0.2025
Guangdong	0.1526	0.1437
Guangxi	0.1405	0.1330
Guizhou	0.1266	0.1189
Hainan	0.1690	0.1549
Hebei	0.1877	0.1795
Heilongjiang	0.1919	0.1885
Henan	0.1487	0.1438
Hubei	0.1353	0.1298
Hunan	0.1270	0.1210
Jilin	0.1908	0.1840
Jiangsu	0.1436	0.1402
Jiangxi	0.1527	0.1345
Liaoning	0.1832	0.1775
Inner Mongolia	0.2273	0.2134
Ningxia	0.2222	0.2043
Qinghai	0.2503	0.2272
Shaanxi	0.1755	0.1638
Shanghai	0.1436	0.1402
Shandong	0.1556	0.1514
Shanxi	0.1983	0.1867
Sichuan	0.1762	0.1642
Tianjin	0.1599	0.1582
Tibet	0.2715	0.2391
Xinjiang	0.2273	0.2106
Yunnan	0.1882	0.1726
Zhejiang	0.1498	0.1411

110 **8. Projected percentage of provincial electricity generation derived from PV in the**  
111 ***Skewed and Balanced* PV deployment scenarios in 2030.**

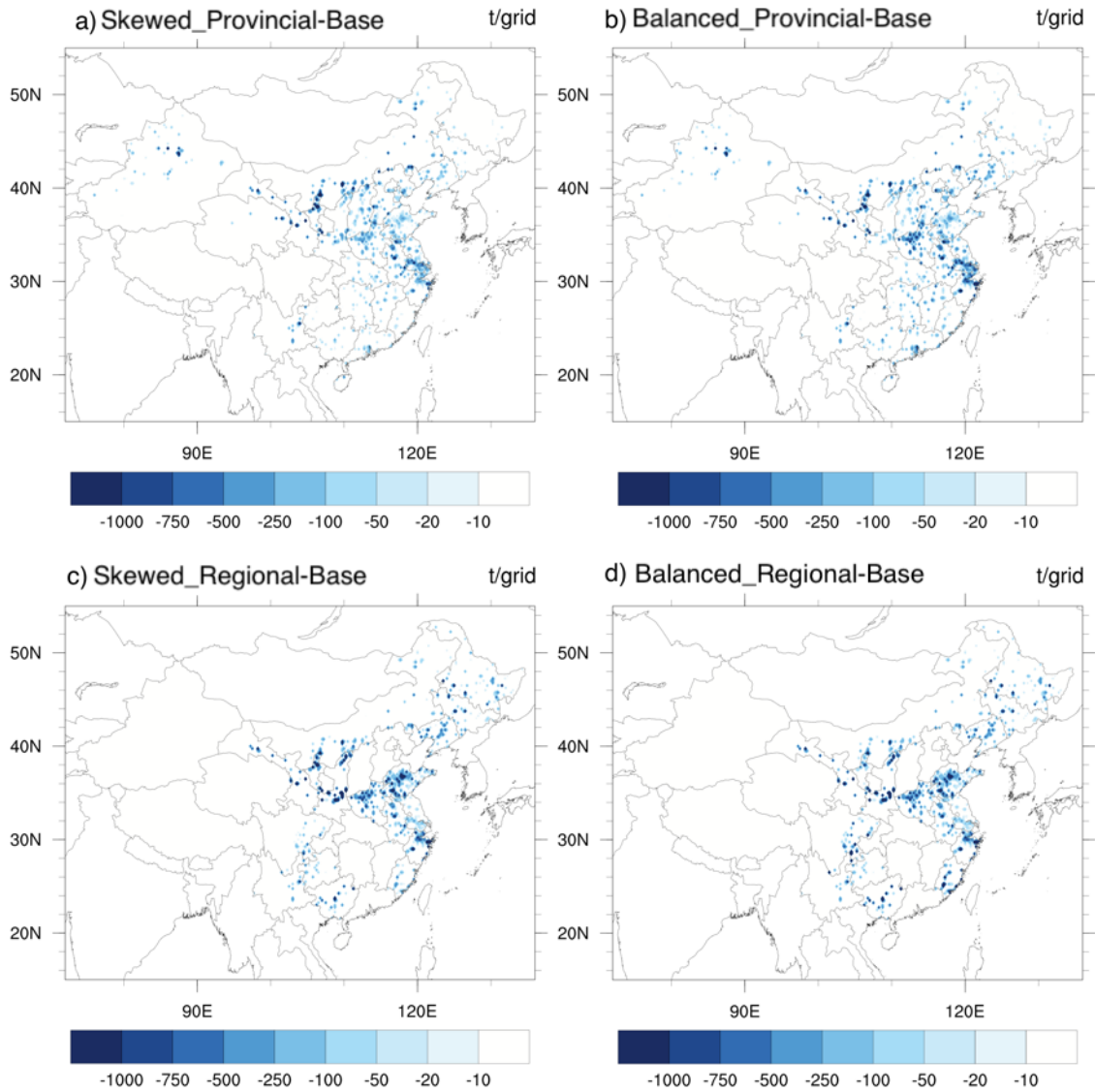
112



113

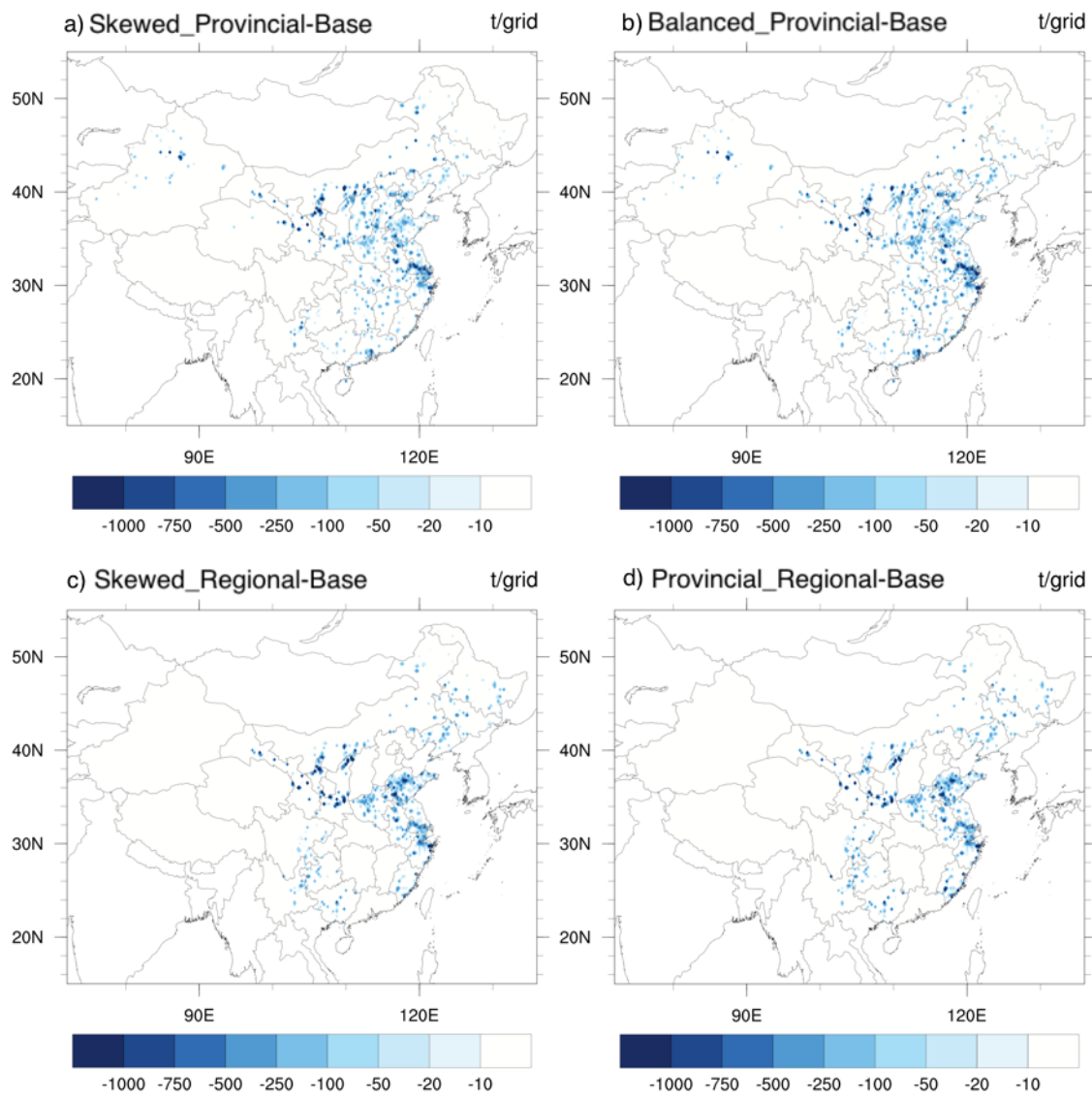
114 **Fig. S2.** Projected percentage of provincial power generation derived from solar PV in  
115 2030.

116 **9. Gridded SO<sub>2</sub> and NO<sub>x</sub> emission reductions in each scenario compared to the base**  
117 **case**



118

119 **Fig. S3.** Gridded annual 2030 SO<sub>2</sub> emission reductions in each scenario (grid size: 0.25  
120 by 0.25 degree) compared to the base case (Base).

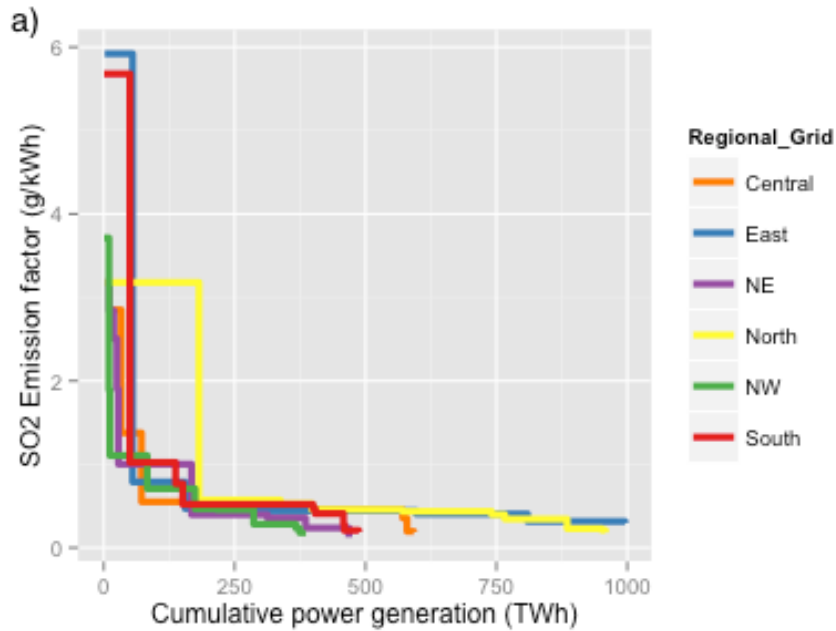


121

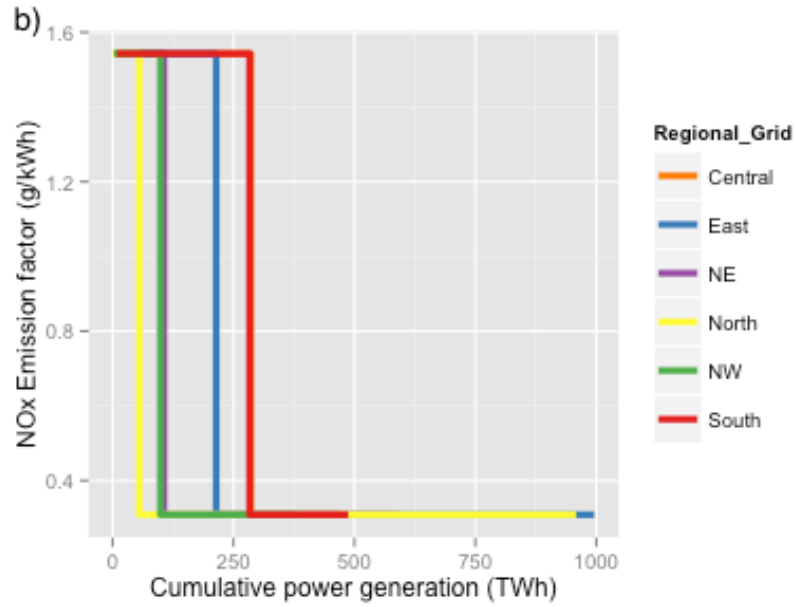
122 **Fig. S4.** Gridded annual 2030 NO<sub>x</sub> emission reductions in each scenario (grid size: 0.25  
 123 by 0.25 degree) compared to the base case (Base).

124 **10. Variations of SO<sub>2</sub> and NO<sub>x</sub> emission factors of coal-fired power plants across**  
125 **regional grids in the 2030 base case and their impacts on emission reduction results.**

126 The criteria we use to determine the order of coal displacement gives more weight to SO<sub>2</sub>  
127 than NO<sub>x</sub> emissions (1.75 to 1 ratio of emission factors) based on their relative  
128 contributions to the formation of secondary aerosols [5]. In addition, SO<sub>2</sub> emission factors  
129 vary more than NO<sub>x</sub> emission factors because of variations in the sulfur content of coal  
130 burned in each province. Therefore coal power plant displacement in our study occurs  
131 predominantly in provinces that have the highest SO<sub>2</sub> emission factors in the power sector  
132 (Fig. S5). Thus, the regional scenarios concentrate coal-fired power plant displacement in  
133 the provinces that have the highest SO<sub>2</sub> emission factors within each regional grid.



134

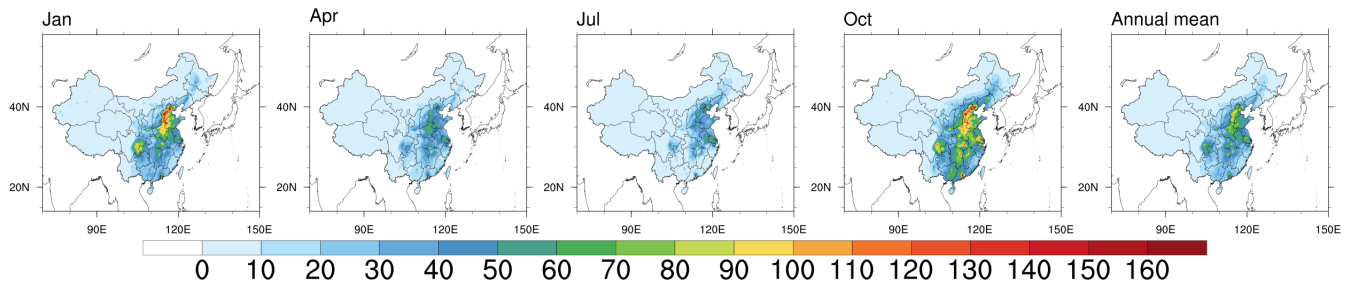


135

136 **Fig. S5.** a) SO<sub>2</sub> and b) NO<sub>x</sub> emission factors of subcritical coal-fired power plants (unit:  
 137 g/kWh) in each regional power grid in 2030 in the ECLIPSE\_v5a\_CLE scenario.

138 Emission factors are plotted from highest to lowest in each regional grid and presented as  
 139 cumulative power generation (TWh) on the x-axis.

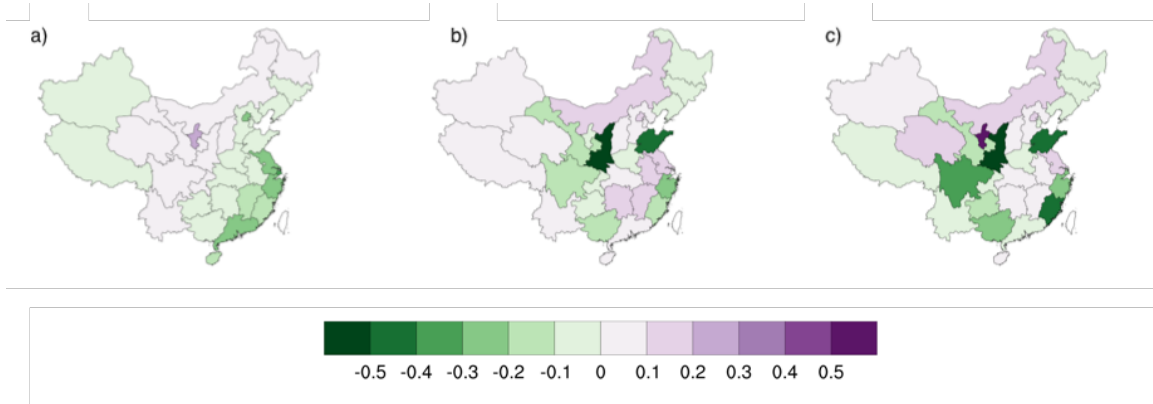
140 **11. 2030 base case monthly and annual mean PM<sub>2.5</sub> concentrations**



141

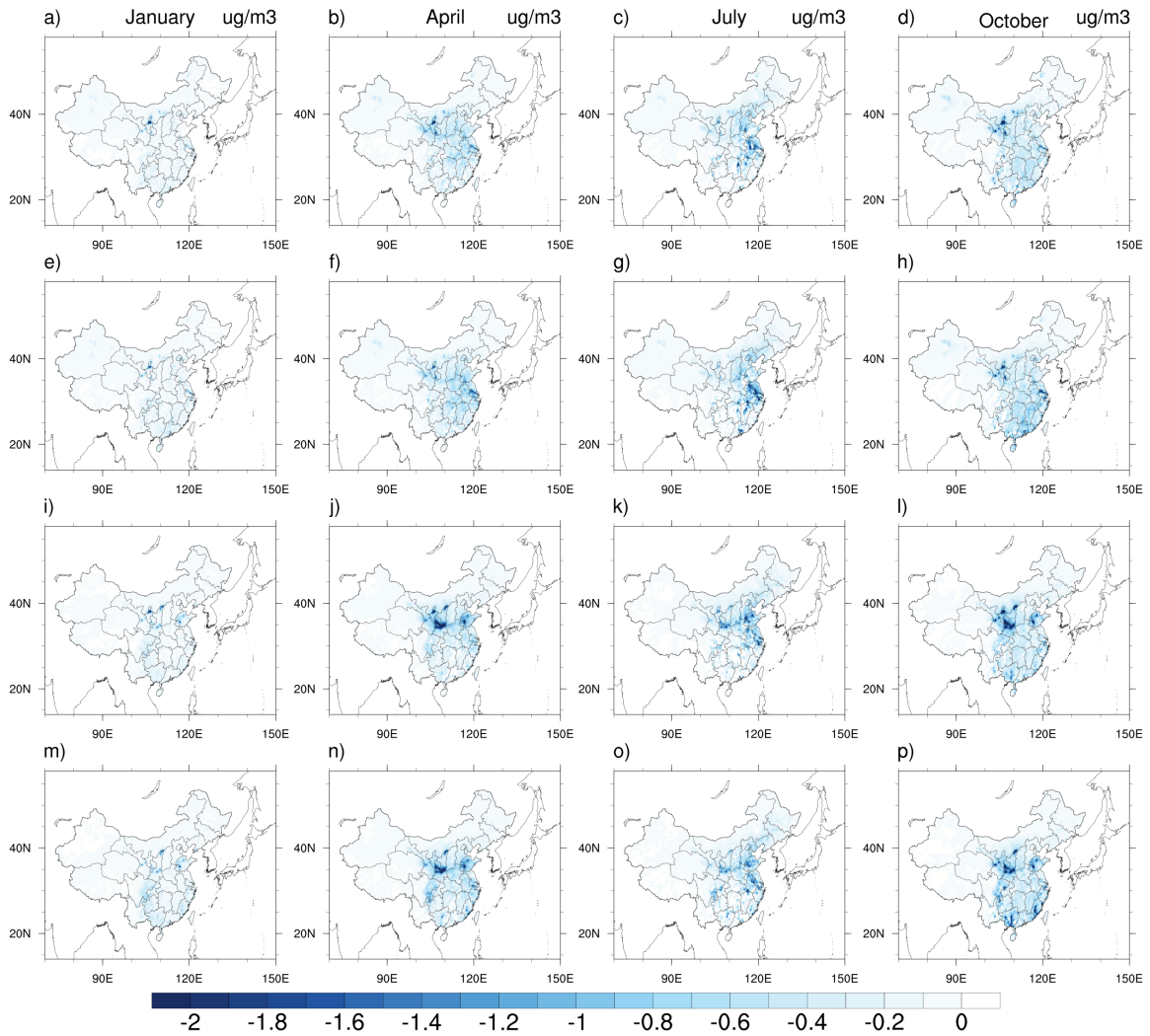
142 **Fig. S6.** 2030 base case monthly and annual mean PM<sub>2.5</sub> concentrations (unit: µg/m<sup>3</sup>).

143 **12. Differences of annual mean  $PM_{2.5}$  concentrations between *Skewed\_Provincial* and**  
144 **other three scenarios**



145 **Fig. S7. a) to c):** Differences between *Skewed Provincial* and the other three scenarios (a)  
146 *Balanced\_Provincial* – *Skewed\_Provincial*; (b) *Skewed\_Regional* – *Skewed\_Provincial*;  
147 (c) *Balanced\_Regional* – *Skewed\_Provincial* (unit:  $\mu\text{g}/\text{m}^3$ ). Purple (green) indicates a  
148 lower (higher) population-weighted  $PM_{2.5}$  in the *Skewed Provincial* scenario than in the  
149 other scenarios.

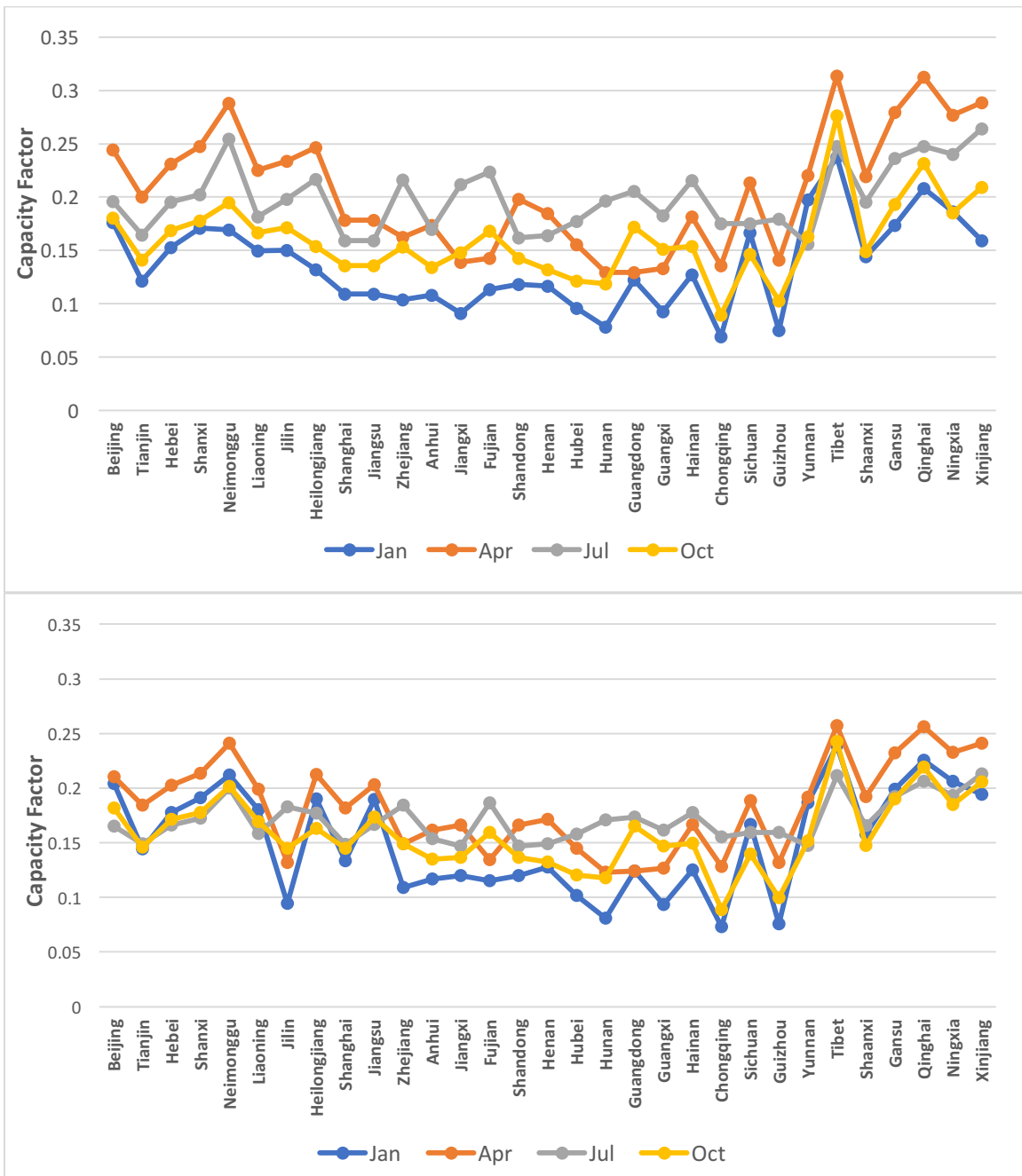
150 **13. Monthly mean PM<sub>2.5</sub> reductions resulting from each PV scenario**



151  
 152 **Fig. S8.** Monthly PM<sub>2.5</sub> reduction in the four PV scenarios compared to the *Base* case. a) to  
 153 d): *Skewed\_Provincial*; e) to h): *Balanced\_Provincial*; i) to l): *Skewed\_Regional*; m) to p):  
 154 *Balanced\_Regional* (unit:  $\mu\text{g}/\text{m}^3$ ).

155  
156

14. Monthly average utility-scale and distributed PV capacity factors



157

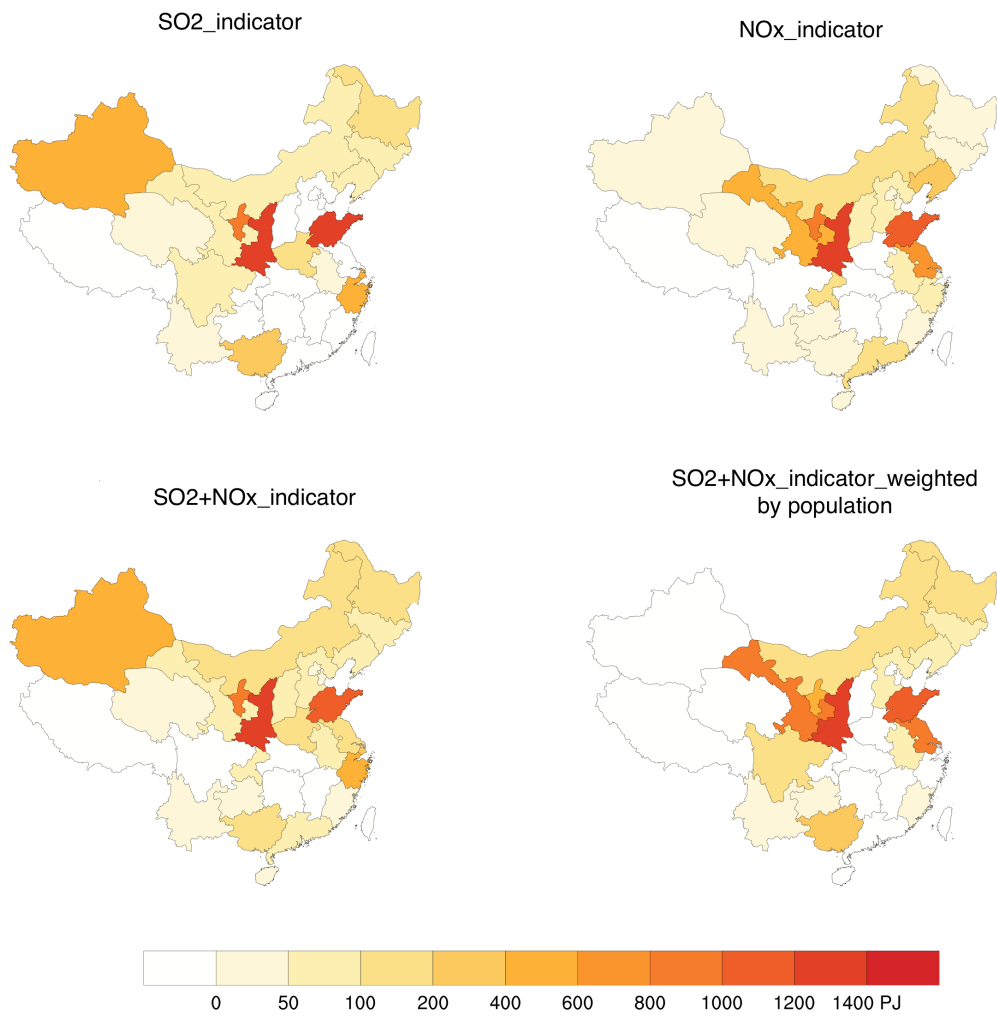
158  
159  
160  
161

Fig. S9. Monthly average utility scale (top) and distributed (bottom) PV capacity factor for each province.

162 **15. Uncertainties in our results**

163 Uncertainties affect our integrated assessment findings regarding: emissions,  
164 displacement strategies, air pollution simulations, and health implications of emission  
165 reductions. For example, the absolute amounts of CO<sub>2</sub> reductions and air quality  
166 improvements are subject to actual 2030 energy consumption and related emissions,  
167 which may deviate from the coal-intensive power sector projection in the base case. In  
168 addition, variations in air pollutant reductions are largely driven by the projected  
169 provincial variations in SO<sub>2</sub> and NO<sub>x</sub> emission factors for coal plants in the base case.  
170 However, our findings that deploying PV in the east with inter-provincial transmission  
171 maximizes the co-benefits would not change since the possibility of displacing the  
172 highest-emitting plants first via transmission and thus resulting in less curtailment in the  
173 east than in the northwest still hold.

174 There are also uncertainties related to the criteria (e.g. damage-weighted PM<sub>2.5</sub> precursor  
175 emissions) used to order the coal power plant displacement. The use of different criteria  
176 will markedly affect the selection of provinces in which coal power plants are displaced  
177 and the resulting emission reductions in each province. Instead of using the coal  
178 displacement rule based on the damage-weighted PM<sub>2.5</sub> precursor emission factors  
179 (1.75\*SO<sub>2</sub> emission factor + NO<sub>x</sub> emission factor) presented in the main results, we test  
180 coal displacement results following three alternative strategies: 1) only using SO<sub>2</sub> as the  
181 indicator (SO<sub>2</sub>\_indicator); 2) only using NO<sub>x</sub> as the indicator (NO<sub>x</sub>\_indicator); 3) using the  
182 1 to 1 ratio of SO<sub>2</sub> and NO<sub>x</sub> emission (SO<sub>2</sub>+NO<sub>x</sub>\_indicator), and 4) using the damage-  
183 weighted PM<sub>2.5</sub> precursor emissions plus also weighted by population density in each  
184 province (SO<sub>2</sub>+NO<sub>x</sub>\_indicator\_weighted by population, calculated as provincial  
185 population divided by the area of the province, unit: person/km<sup>2</sup>) [3]. We use the Skewed  
186 deployment pattern with inter-provincial PV electricity transmission as the example to  
187 show the difference. As shown in Fig. S10, the provinces where significant coal  
188 displacement occurs vary depending on the indicator used. Thus the displacement  
189 strategy employed is critical in determining the emission reduction benefits of solar PV.



190  
191

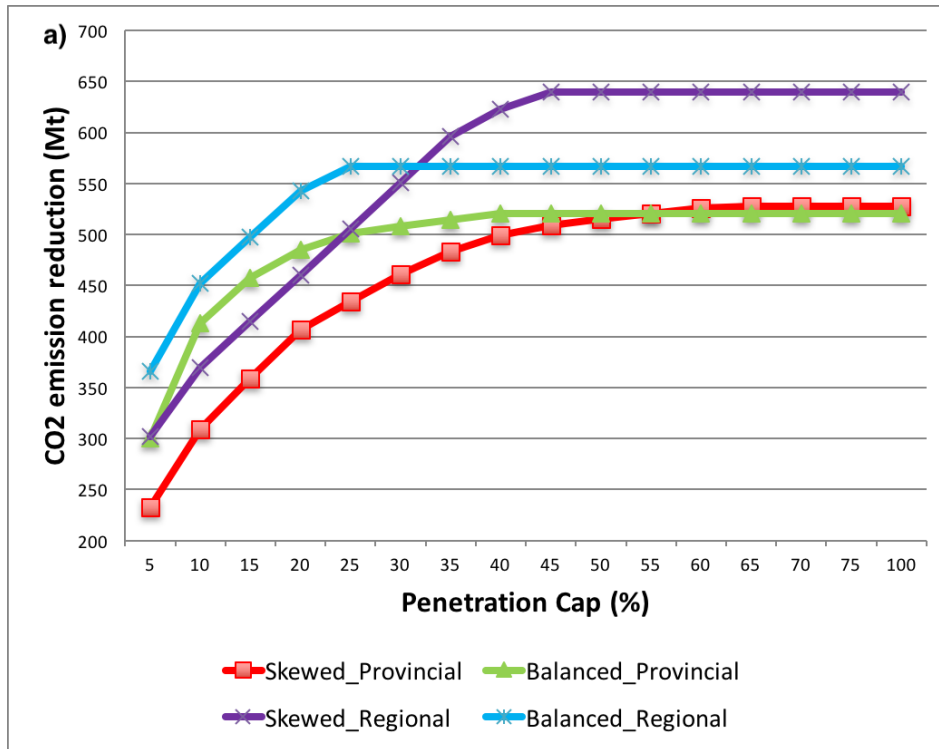
**Fig. S10.** Coal displacement results (unit: PJ) using different coal displacement metrics

192 **16. Sensitivity analysis of the implications of various levels of PV grid integration**

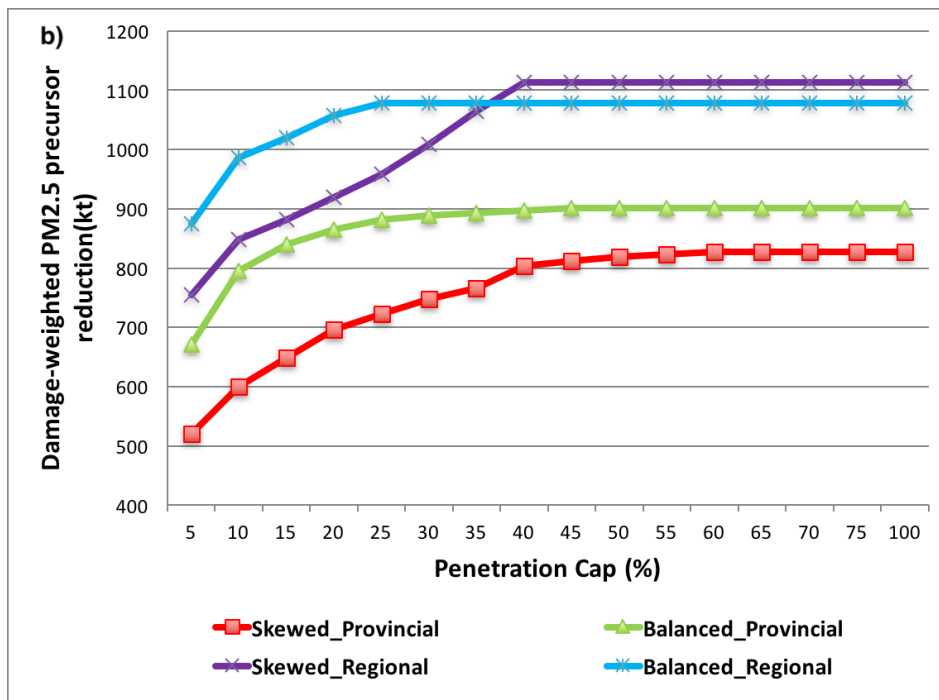
193 In our analysis in the main results, we imposed a cap on PV penetration of 30% for each  
194 province or grid, depending on the scenario. Here we conduct a sensitivity analysis  
195 evaluating the impact of a range of PV penetration caps (from 5% up to 100%) on grid-  
196 integrated PV electricity generation, carbon and air pollutant emission reductions (Fig.  
197 S11). We find that enabling inter-provincial PV electricity transmission in the *Regional*  
198 scenarios always results in more CO<sub>2</sub> and damage-weighted PM<sub>2.5</sub> precursor reductions  
199 (calculated as 1.75\*SO<sub>2</sub> + NO<sub>x</sub>) compared to the *Provincial* scenarios without inter-  
200 provincial transmission. This indicates that inter-provincial transmission not only reduces  
201 the grid-integration constraints of PV, but also effectively prioritizes the displacement of  
202 less efficient and more high-emitting coal-fired power plants. If we only utilize PV  
203 electricity within the province where it is generated, some supercritical or ultra-  
204 supercritical power plants with higher generation efficiency and more advanced pollution  
205 control technologies will be displaced.

206 The results vary slightly for deploying distributed PV in the east. Without inter-provincial  
207 transmission, deploying more distributed PV in the east (*Balanced\_Provincial*) always  
208 leads to greater CO<sub>2</sub> and PM<sub>2.5</sub> precursor reductions than deploying more utility-scale PV  
209 in the northwest (*Skewed\_Provincial*), regardless of the allowed maximum PV grid  
210 penetration. This is because the eastern provinces contain more high emitting power  
211 plants than the west and because without transmission lower-emitting and higher  
212 efficiency coal power plants in the west will be displaced with PV. However, with inter-  
213 provincial transmission, deploying more utility-scale PV in the northwest achieves  
214 greater CO<sub>2</sub> and air pollutant emission reductions once the penetration cap rises above  
215 35%, primarily because increasing grid-integrated PV electricity generation is possible  
216 after relaxing the grid-integration constraints. This suggests that dramatic expansion of  
217 power transmission that alleviates the grid-integration constraints would allow  
218 deployment of solar PV in provinces with the most abundant solar radiation and the  
219 delivery of PV electricity to provinces with the highest emission reduction potential,  
220 which would further increase the health and climate co-benefits of PV.

221



222



223

224 **Fig. S11.** (a) CO<sub>2</sub> and (b) damage-weighted PM<sub>2.5</sub> precursor (1.75\*SO<sub>2</sub> + NO<sub>x</sub>) reductions  
 225 resulting from various PV penetration caps for each scenario.

226

227

228

229 **17. Applicability of the integrated assessment framework used in this study to**  
230 **analyze the co-benefits of solar PV in other countries**

231 In our study, we develop an integrated assessment framework to quantify the climate, air  
232 quality and related human benefits of solar PV generation in China. Our findings for  
233 China are consistent with previous findings in the US that suggest that installing solar PV  
234 panels in locations with the highest insolation and hence largest electricity generation  
235 may not generate the largest environmental benefits as these benefits depend heavily on  
236 local demand, available transmission and what power generation is displaced [6]. This  
237 framework used in our study could also be applied to studies of the co-benefits of solar  
238 PV in other countries facing similar grid-integration constraints and mismatch between  
239 PV generation and electricity demand. For example, there is growing recognition in India  
240 that concentrating PV generation in the states with the best solar resources will  
241 exacerbate grid integration constraints and a significant transmission investment is  
242 needed to increase environmental co-benefits [7]. Our integrated assessment framework  
243 could be used to quantify the air quality and climate co-benefits of various PV  
244 deployment scenarios in India and other countries.

245

246 **References:**

- 247 1. Li X, Wagner F, Peng W, Yang J and Mauzerall D L (2017) Reduction of solar  
248 photovoltaic resources due to air pollution in China *Proc. Natl Acad. Sci.* 114(45), 18867.
- 249 2. Buonocore JJ, Dong X, Spengler JD, Fu JS & Levy JI (2014) Using the community  
250 multiscale air quality (CMAQ) model to estimate public health impacts of PM 2.5 from  
251 individual power plants. *Environ Int* 68: 200-208.
- 252 3. All China Marketing Research Co. Ltd. (2014) China census data by county, 2000-  
253 2010. [http://map.princeton.edu/search/details/#/9107c437-8169-4444-9427-](http://map.princeton.edu/search/details/#/9107c437-8169-4444-9427-3b6957a09bca)  
254 [3b6957a09bca](http://map.princeton.edu/search/details/#/9107c437-8169-4444-9427-3b6957a09bca). Accessed March 6, 2017.
- 255 4. Burnett RT, *et al* (2014) An integrated risk function for estimating the global burden of  
256 disease attributable to ambient fine particulate matter exposure. *Environ Health Perspect*  
257 122(4): 397-403.

258 5. Buonocore JJ, Dong X, Spengler JD, Fu JS, Levy JI. Using the Community Multiscale  
259 Air Quality (CMAQ) model to estimate public health impacts of PM 2.5 from individual  
260 power plants. *Environ Int* 2014;68:200-208.

261 6. Siler-Evans K, Azevedo IL, Morgan MG, Apt J. Regional variations in the health,  
262 environmental, and climate benefits of wind and solar generation. *Proc Natl Acad Sci U S*  
263 *A* 2013 Jul 16;110(29):11768-11773.

264 7. Bridge to India. India's first wind power auction to upend traditional business model.  
265 Available at [www.bridgetoindia.com/indias-first-wind-power-auction-upend-traditional-](http://www.bridgetoindia.com/indias-first-wind-power-auction-upend-traditional-business-model)  
266 [business-model](http://www.bridgetoindia.com/indias-first-wind-power-auction-upend-traditional-business-model). Accessed March 6, 2017.

267